High Energy Physics and Nuclear Physics

Volume 20, Number 2

Multichannel Fission Model Applied to ^{233,235,238}U(n,f)

Fan Tieshuan, Hu Jimin, and Bao Shanglian

(Department of Technical Physics, Peking University, Beijing, China)

In the frame of the multichannel fission and random neck rupture model, the fragment mass, average kinetic energy distributions, and the neutron multiplicities of the neutron-induced fissions of ^{233,235,238}U are calculated covering the incident neutron energy range from thermal to 6 MeV. The theoretical results are in accord with the experimental data. The dependence of the fission channel probability on the excitation energy has been investigated.

Key words: random neck rupture, multichannel fission model, fission mechanism.

1. INTRODUCTION

It is a difficult and interesting task to understand the induced fission mechanism of uranium isotopes. The multichannel fission and random neck rupture model [1,2] has aroused wide interests of nuclear physicists because it achieved remarkable successes in investigating the exit-channel observables of the low-energy neutron induced and spontaneous fissions and deep-inelastic collisions since the 1980s.

The multichannel fission model (or multi-mode fission model) is gradually developed from analyzing the experimental results of the post-scission phenomena. The model can be easily applied to the analysis of the empirical mass distribution of actinide nuclei and quantitatively in good accord with the experimental data [3]. On the contrary, the other models (e.g., the statistical model) give only qualitative or semi-quantitative agreement with the experiment [4]. It is unfortunate that the

Received on April 3, 1995. Supported by the Foundation from the Ph.D. Program of High Education of China and Nuclear Science Foundation of China National Nuclear Corporation.

© 1996 by Allerton Press, Inc. Authorization to photocopy individual items for internal or personal use, or the internal or personal use of specific clients, is granted by Allerton Press, Inc. for libraries and other users registered with the Copyright Clearance Center (CCC) Transactional Reporting Service, provided that the base fee of $50.00 per copy is paid directly to CCC, 222 Rosewood Drive, Danvers, MA 01923.

multichannel fission model has a weak theoretical basis. In fact, this model is applied to analyzing the fragment mass distributions only by using several Gaussian functions to fit the experimental data of mass distributions. From the model itself, the prescission shapes of the compound nucleus cannot be obtained and other fragment properties, such as total kinetic energy distributions, could not be studied. Brosa, Grossmann, and Moller [1] have computed the potential energy surface from the ground state up to the scission point for actinide nuclei using Strutinstky's approach, their results show the presence of different numbers of fission channels or paths on the potential energy surface for different fissioning nuclei. They also obtained the prescission shapes corresponding to the fission channels of the compound nuclei and computed some properties of the fission channels of the compound nuclei and computed some properties of the fission fragments by combining the multichannel model with the random neck rupture approximation.

We consider that for the study of fragment properties of the neutron-induced fissions, it is still the most hopeful procedure to use the multichannel fission and random neck rupture model. However, it is better to obtain the reasonable prescission shapes before proceeding quantitative calculations. At present, it is difficult to obtain the reasonable prescission shapes only from this theory. This work is based on the hypothesis that there are several fission channels for one fissioning system, and different semi-empirical prescission shapes for different fission channels are adopted. The study of the post-scission phenomena has been proceeded according to the following steps: 1) the prescission shapes for different fission channels are determined. 2) In accordance with the random neck rupture, the fragment mass, total kinetic energy distributions, and neutron multiplicities for each channel are calculated for the given prescission shapes. 3) The channel probabilities, which represent the relative populations of the fission modes, are computed. 4) The calculated fragment mass, total kinetic energy distributions, neutron multiplicities, and the total kinetic energy distributions for a fixed mass fragment are obtained by the superposition of various channels. In Ref. 2, for the neutron-induced fission of ^{235}U covering the incident neutron energy range from thermal to 6 MeV, the mass and total kinetic energy distributions for the fission fragments are calculated assuming the presence of three fission channels and the dependence of the channel probabilities on the excitation energies is investigated. The calculated results are in agreement with the empirical data.

2. CALCULATIONS OF THE MASS, AND KINETIC ENERGY DISTRIBUTIONS FOR FISSION FRAGMENTS

The prescission shapes are made of two relatively large heads connected by a long, thick neck, where the smooth connection of both heads and the neck is realized by a hyperboloid of revolution. The shape equation similar to the one in Ref. 2 has been chosen, where its representation contains 9 parameters (l, r, z, c, a, r_1, r_2, ζ_1, and ζ_2) whose meanings can be seen in Ref. 2. Using the shape parameters for ^{235}U(n,f) obtained by us, the semi-length l and neck radius r of the prescission shape for ^{233,238}U(n,f) can be approximated through the following equations:

$$l=(A_{cn}/A_{cn0})^{1/3}\cdot\ l_0\ , \tag{1}$$

$$r=(A_{cn}/A_{cn0})^{1/3}\ \cdot\ r_0\ . \tag{2}$$

where the mass number of the compound nucleus A_{cn0}, the semi-length l_0 and the neck radius r_0 of the prescission shape are for ^{235}U(n,f), and those parameters without subscript 0 for ^{233,238}U(n,f). The position z of the narrowest point and the curvature c of the neck can be obtained by analyzing the empirical mass distributions of the fission fragments. A set of five equations can be obtained by requiring the prescission shape function continuous and continuously differentiable at the transitional points and the volume conservation of the fissioning nucleus. By solving it, the values of parameters a, r_1, r_2, ζ_1, and ζ_2 can be determined.

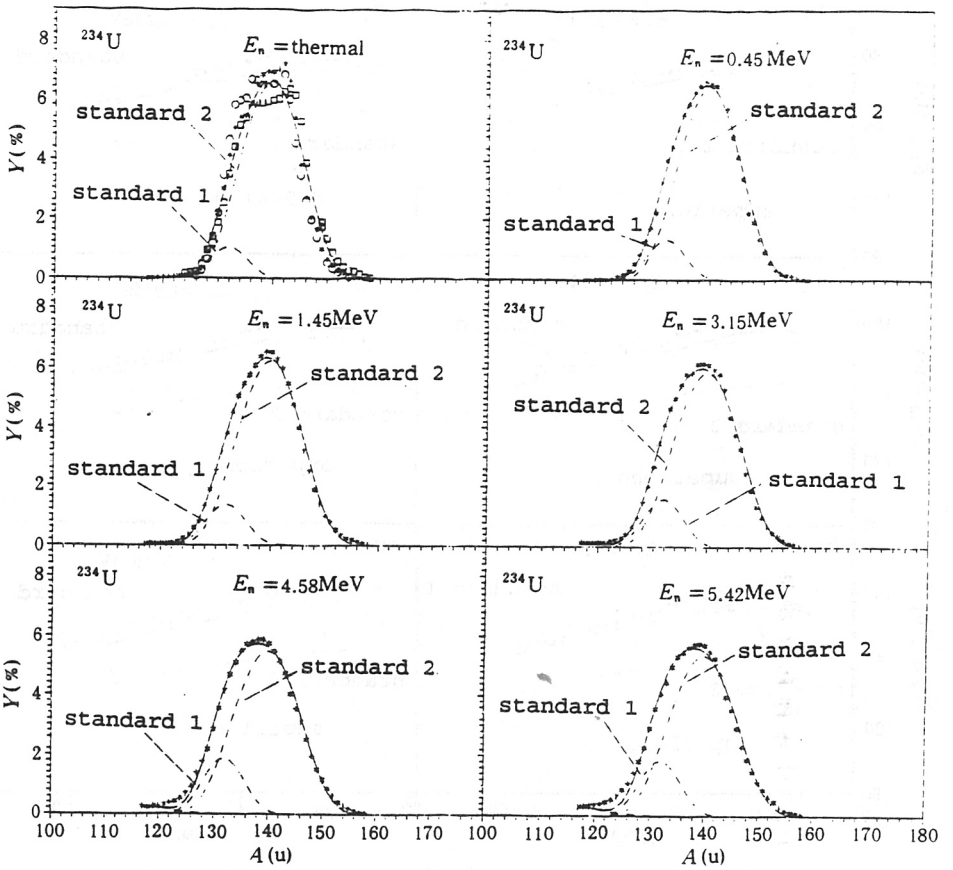

Fig. 1
The comparison between the calculated and experimental mass distributions [6-10] of the fission fragments for ^{233}U(n,f) at E_n = thermal, 0.45, 1.45, 3.15, 4.58, and 5.42 MeV.

The distribution probabilities of each fission channel for ^{233}U(n,f) and ^{238}U(n,f) are obtained by fitting the empirical data of the mass distributions of the fission fragments. The results indicate that for the low energy neutron-induced fissions of uranium isotopes, the standard 2 channel which represents the properties of the asymmetric fission component is the most important fission channel, and the superlong channel corresponding to symmetric fission will rapidly increase with the increase of the incident neutron energy. The above-mentioned trends are in accordance with the results given from the other authors [1,3,5] who have conducted the multi-mode analyses for the fragment mass distributions.

Based on both the obtained prescission shapes and the channel probabilities and using the calculating methods and equations similar to those in Ref. 2, the mass and average total kinetic energy distributions of the fission fragments for ^{233,238}U(n,f) have been calculated and compared with measurements. For ^{233}U(n,f), the covering range of the incident neutron energy is E_n = thermal, −5.50 MeV and for ^{238}U(n,f), E_n = 1.3–5.3 MeV. As an example, Fig. 1 shows the calculated fragment mass distributions for ^{238}U(n,f) with the incident neutron energy E_n = thermal, 0.45, 1.45, 3.15, 4.58, and 5.42 MeV. The calculated mass distributions are in agreement with the empirical ones. The results of theoretical calculations also indicate that for the same fissioning system for at different incident neutron

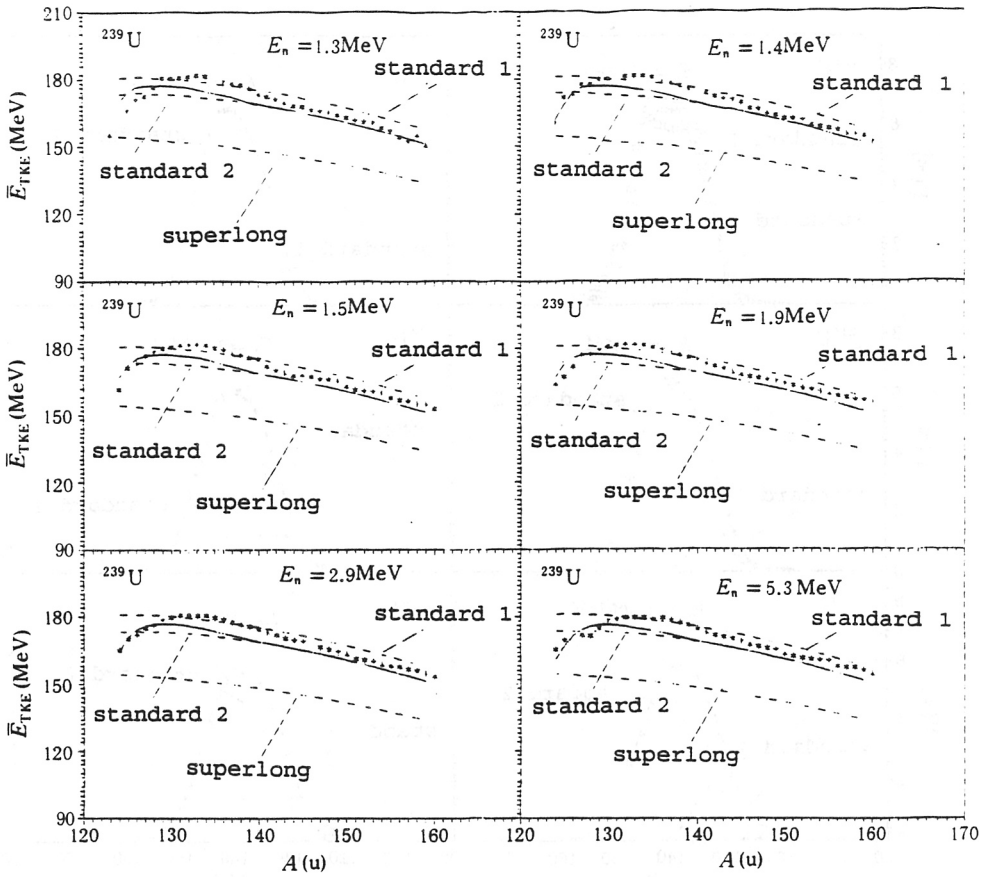

Fig. 2

The comparison between the calculated and experimental results [11] of the average kinetic energy distributions of the fragments for ^{238}U(n,f) at E_n = 1.3, 1.4, 1.5, 1.9, 2.9, and 5.5 MeV.

energies, the most probable mass of the fragment mass distribution for each channel will keep the same value while the semi-width of the mass distribution for each channel changes. This results should not take us by surprise because the same prescission shape of the compound nucleus has been used for different incoming neutron energies.

Figure 2 illustrates the calculated and experimental results of the average total kinetic energy distributions of the fragments for neutron-induced fission of ^{238}U with E_n = 1.3, 1.4, 1.5, 1.9, 2.9, and 5.3 MeV. The calculated total kinetic energy distributions of the fragments do not evidently change with the change of the incoming neutron energy, which conforms to a large number of experimental measurements.

3. CALCULATIONS OF NEUTRON MULTIPLICITIES

When the nucleus scissions happen at different positions on the neck of the prescission shape, the fragments can be approximately represented by touching ellipsoids, as a result of the effect of the strong surface tension [1]. At first, these newborn fragments are in high excitation states and the

excitation energy release is dissipated by emission of neutrons and γ-rays. If the emission of the prescission neutrons is neglected, the main portion of the fission neutrons are emitted during the process of the fragment deexcitation. The emission of the few neutrons which follow β-decay of the primary fission fragments is not considered because their characteristics are not directly related to the fission mechanism.

If a_1, b_1, a_2, and b_2 represent the major and minor semi-axes of both complementary fragments, respectively, they can be written as

$$a_1=(r_1+z_r)/2, \quad b_1^2=3/(4a_1)\int_{-r_1}^{z_r}\rho^2\,d\zeta\ , \tag{3}$$

$$a_2=l-a_1, \qquad b_2^2=3/(4a_2)\int_{z_r}^{2l-r_1}\rho^2\,d\zeta\ , \tag{4}$$

where l is the semi-length of the prescission shape, Z_r and r_1 are the arbitrary rupture position on the neck and the radius of the left semi-sphere, respectively. The eccentricities ε of the fragments are evaluated using the following formula

$$\varepsilon=[1-(b_i/a_i)^2]^{1/2} \qquad i=1,2. \tag{5}$$

The nascent fragments contain both the internal excitation energy of the fissioning nucleus before scission and the excitation energy into which the deformation energy is transferred from the decay of the collective motion. The large amount of experimental data indicates that the energy cost of one neutron emission of the fission fragments is about 8 MeV. Therefore, the theoretical neutron multiplicity can be calculated as

$$\bar{\nu}(A)=\sum_{i=1}^{3} W_i E_i^*(A)\,Y_i(A)/(8Y(A)), \tag{6}$$

The index i = 1, 2, 3 is for the standard 1, standard 2, and superlong channels, W_i the probability for channel i, $Y_i(A)$ and $Y(A)$ are the mass distributions for the i-th channel and the superposition of the mass distributions for three channels; the available excitation energy in the fragment with the mass number A for the i-th channel, $E_i^*(A)$ can be calculated by the following formula

$$E_i^*(A)=E_{s,i}^*\,A/A_{cn}+E_{def,i}(A), \tag{7}$$

where

$$E_{s,i}^*=\kappa(E_{des,i}+B_n)+E_n\ . \tag{8}$$

The first term in Eq.(7) is the share of the thermal energy received by the fragment with mass number A from the prescission nucleus A_{cn}. $E_{def,i}$ is the potential energy difference between the prescission shape and the spherical shape for channel i, obtained from Table 8.5 in Ref. 1. B_n is the binding energy of the last neutron of the compound nucleus and E_n the kinetic energy of the incident neutron. The factor $\kappa\sim0.26$ is the fraction of $(E_{def,i}+B_n)$ transferred into the internal excitation, which is related to the odd-even effects in fission [12,13].

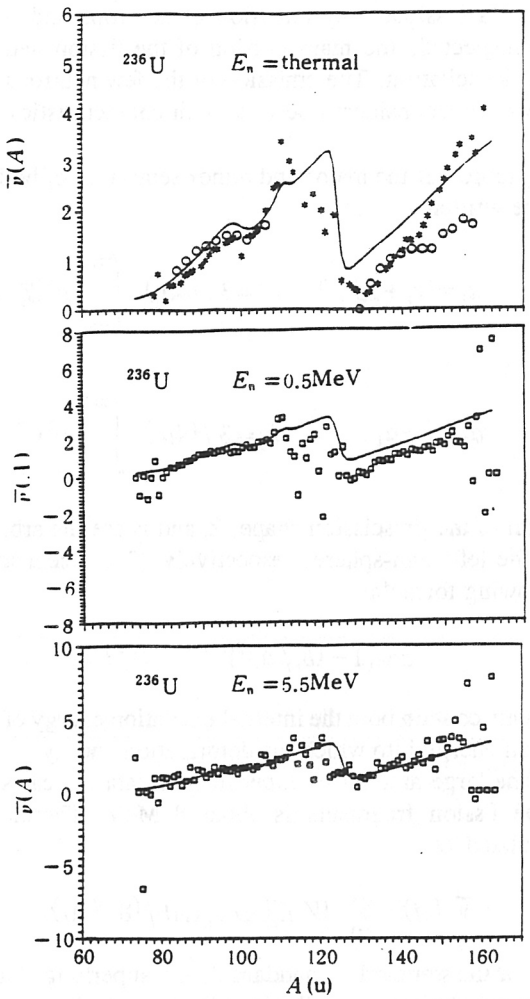

Fig. 3

The comparison between the calculated and experimental results of the neutron multiplicities for ^{235}U(n,f) at E_n = thermal, 0.5, and 5.5 MeV.

The second term in Eq.(7) represents the deformation energy of the fragment with the mass number A, for any fission channel it can be calculated by

$$E_{def}(A) = E_{sur}^{sph}(A) \times \left\{ \frac{\arcsin\ \varepsilon + \varepsilon(1-\varepsilon^2)^{1/2}}{2\varepsilon(1-\varepsilon^2)^{1/6}} - 1 + 2\chi\left[\frac{(1-\varepsilon^2)^{1/3}}{2\varepsilon} \ln \frac{1+\varepsilon}{1-\varepsilon} - 1 \right] \right\}. \quad (9)$$

with the fissility χ obtained from the following equations

$$\chi = E_{cou}^{sph}(A) / (2E_{sur}^{sph}(A)), \quad (10)$$

Table 1
The theoretically calculated and experimental results [16,17] of the neutron multiplicities.

Compound nuclei	E_n (MeV)	$\bar{\nu}_{st2}$	$\bar{\nu}_{st1}$	$\bar{\nu}_{s1}$	$\bar{\nu}$	$\bar{\nu}_{exp}$
^{234}U	Thermal	3.28	2.39	4.45	3.20	2.50
	5.5	3.97	3.01	5.08	3.78	3.12
^{236}U	Thermal	3.16	2.30	5.55	2.99	2.43
	0.5	3.23	2.36	5.64	3.06	2.73
	5.5	3.85	2.99	6.23	3.67	3.19
^{239}U	1.5	2.98	2.25	5.24	2.87	2.56
	5.5	3.57	2.74	5.80	3.38	3.17

Table 2
The analyzing results for the fragment properties of the thermal neutron-induced fissions of ^{235}U.

Authors	Fission channels	Channel probabilities [%]	The most probable mass [u]	Widths of mass distributions [u]	Total kinetic energies [MeV]	Prompt neutron number
Knitter	standard 2	81.4	141.1	4.96	167±1	
	standard 1	18.3	133.9	2.63	187±1	
	superlong	0.07	118	4.13	157±7	
Brosa	standard 2		147±5	5.9±4	151±4	2.0
	standard 1		133±5	3.4±1	183±6	2.9
	superlong		118±5	5.5±4	159±4	7.3
F.C. Wang	standard 2	78.0	140.7	5.10		
	standard 1	18.0	133.9	2.35		
	superlong	0.2	118	7.14		
This work	standard 2	82.1	140.6	4.53	168.3	3.16
	standard 1	17.8	133.1	2.47	180.6	2.30
	superlong	0.1	118.0	4.88	157.0	5.55

$$E_{cou}^{sph}(A) = 0.7053Z^2 / A^{1/3}\text{MeV},$$

$$E_{sur}^{sph}(A) = 17.944[1 - 1.7826 \tag{11}$$

$$[(N-Z)/A]^2]\ A^{2/3}\text{MeV}, \tag{12}$$

$$A = A(A_{cn}/Z_{cn})(Z-0.5), \tag{13}$$

$$A - A_{cn} = (A_{cn}/Z_{cn})(Z_{cn} - Z + 0.5), \tag{14}$$

where $E_{cou}^{sph}(A)$ and $E_{sur}^{sph}(A)$ represent the Coulomb and surface energies of a spherical nucleus, A, Z, A_{cn}, and Z_{cn} the mass number and charge number of the fragments and the compound nucleus, respectively.

For different incident neutron energies, the neutron multiplicities for ^{233,238}U(n,f) have been calculated using Eqs.(3)-(14), with the numerical results listed in Table 1, where $\bar{\nu}_{st1}$, $\bar{\nu}_{st2}$ and $\bar{\nu}_{sl}$ are the prompt neutron number distributions for standard 2, standard 1, and superlong channels, $\bar{\nu}$ and $\bar{\nu}_{exp}$ are the average number of neutrons per fission obtained from calculations and experiments, respectively. As an example, in Fig. 3, the neutron multiplicities of ^{235}U(n,f) as a function of the fragment mass obtained from our calculations are illustrated for thermal neutrons and the neutrons of E_n = 0.5 MeV and 5.5 MeV, together with the experimental results [9,14,15] as a comparison. From the given figure and table, we can see that the calculated values of neutron multiplicities are higher than the empirical ones though the trends of them are generally consistent. To carefully adjust the semi-length l of the prescission shapes of the fission nucleus may effects the results to some extent, but it seems that the excitation energy of 1–2 MeV should be transferred to other degrees of freedom.

4. CONCLUSIONS

The main post-scission phenomena of the neutron-induced fissions of ^{233}U, ^{235}U, and ^{238}U have been systematically studied using the improved multichannel and random neck rupture fission model. By connecting several main parameters of prescission shape with suitable fragment properties, a method for calculating prescission shape parameters of the fissioning nucleus is presented. This method has been used to calculate the fragment mass, total kinetic energy, and the prompt neutron distributions of the fissioning system. It is believed that the prescission shape obtained by the above-mentioned method in a certain degree can avoid the arbitrariness, considering the certain internal relations existed in the properties of the fission fragments.

Table 2 is given in order to compare our theoretical calculations with studies of the fragment properties by other authors. H.H. Knitter *et al.* [18] have given a formula for fragment mass distribution as a function of the fragment mass and total kinetic energy and then by fitting to experimental data obtained the fragment mass and total kinetic energy distributions for the thermal neutron-induced fission of ^{235}U. Their calculations can be in good agreement with the measurements. Wang and Hu [3] analyzed the fragment mass distributions of main actinide isotopes by fitting 5 Gaussian functions to the empirical data and obtaining the channel probabilities from the measurements. Brosa *et al.*'s theoretical calculations [1,18] indicate the existence of channels and give the general characteristics of the fragment mass, kinetic energy, and neutron distributions. The present work has given both the channel probabilities and prescission shapes for each fission channel and studied the main fragment properties, with results being generally consistent to other works.

REFERENCES

[1] U. Brosa, S. Grossmann, and A. Moller, *Phys. Repts.*, **197**(1990), p. 167.
[2] Fan Tieshuan, Hu Jimin, Bao Shanglian, *High Energy Phys. and Nucl. Phys.* (in Chinese), Supp. **18**(1994), p. 47.
[3] Wang Fucheng and Hu Jimin, *J. Phys.*, **G15**(1989), p. 829.
[4] A. Wilkins, E.P. Steinberg, and R.R. Chasman, *Phys. Rev.*, **C14**(1976), p. 1832.
[5] F.J. Hambsch *et al.*, *Nucl. Phys.*, **A491**(1989), p. 56.
[6] V.M. Surin *et al.*, *Yad. Fiz.*, **14**(1971), p. 935.
[7] F. Pleasonton, *Phys. Rev.*, **174**(1968), p. 1500.
[8] S. Katocoff, *Nucleonics*, **18**(1960), p. 201.
[9] J. Terrell *et al.*, *Phys. Rev.*, **127**(1962), p. 880.
[10] A.I. Sergachev *et al.*, *Yad. Fiz.*, **16**(1972), p. 475.
[11] V.G. Vorobyeva *et al.*, *Yad. Fiz.*, **9**(1969), p. 296.
[12] N. Nifenecker *et al.*, *Z. Phys.*, **A308**(1982), p. 39.

[13] F.J. Gonnenwein, *Radiation Effects*, **94**(1986), p. 205.
[14] V.A. Apalin *et al.*, *Nucl. Phys.*, **71**(1965), p. 553.
[15] A.A. Naqiv *et al.*, *Phys. Rev.*, **C34**(1986), p. 218.
[16] G.D. James *et al.*, *Nuclear Fission and Neutron-Induced Fission Cross Sections*, Pergamon Press, Oxford, 1981, p. 24.
[17] F. Manero *et al.*, *At. Energy Rev.*, **10**(1972), p. 637.
[18] H.H. Knitter *et al.*, *Z. Naturforsch*, **A42**(1987), p. 786.